



ELSEVIER

Contents lists available at ScienceDirect

Ecotoxicology and Environmental Safety

journal homepage: www.elsevier.com/locate/ecoenv

Biosorption and biodegradation of pyrene by *Brevibacillus brevis* and cellular responses to pyrene treatment

Liping Liao^a, Shuona Chen^a, Hui Peng^b, Hua Yin^{c,*}, Jinshao Ye^{a,*}, Zehua Liu^c, Zhi Dang^c, Zhichen Liu^a

^a Department of Environmental Engineering, Jinan University, Guangzhou 510632, China

^b Department of Chemistry, Jinan University, Guangzhou 510632, Guangdong, China

^c Key Laboratory of Ministry of Education on Pollution Control and Ecosystem Restoration in Industry Clusters, College of Environment and Energy, South China University of Technology, Guangzhou 510006, Guangdong, China

ARTICLE INFO

Article history:

Received 14 October 2014

Received in revised form

7 February 2015

Accepted 8 February 2015

Available online 18 February 2015

Keywords:

Pyrene

Biodegradation

Biosorption

Brevibacillus brevis

Cellular responses

Flow cytometry

ABSTRACT

Biodegradation has been proposed as an effective approach to remove pyrene, however, the information regarding cellular responses to pyrene treatment is limited thus far. In this study, the biodegradation and biosorption of pyrene by *Brevibacillus brevis*, along with cellular responses caused by pollutant were investigated by means of flow cytometry assay and scanning electron microscopy. The experimental results showed that pyrene was initially adsorbed by *B. brevis* and subsequently transported and intracellularly degraded. During this process, pyrene removal was primarily dependent on biodegradation. Cell invagination and cell surface corrugation occurred due to pyrene exposure. Nevertheless, cell re-growth after 96 h treatment was observed, and the proportion of necrotic cell was only 2.8% after pyrene exposure for 120 h, confirming that *B. brevis* could utilize pyrene as a sole carbon source for growth. The removal and biodegradation amount of pyrene (1 mg/L) at 168 h were 0.75 and 0.69 mg/L, respectively, and the biosorption amount by inactivated cells was 0.41 mg/L at this time.

© 2015 Elsevier Inc. All rights reserved.

1. Introduction

Pyrene is less bioavailable and more resistant to biological attacking as a typical high-molecular weight polycyclic aromatic hydrocarbon (PAH) (Dissanayake et al., 2010). With wide distribution in the aquatic environment, pyrene, which is toxic to human and organisms, represents a major portion of the total PAHs found in contaminated sites (Oliveira et al., 2012). Compared with sorption, photolysis or chemical oxidation, biodegradation is commonly believed as a more effective approach to remove pyrene from the aquatic environment (Das and Mukherjee, 2007).

Typically, biosorption and biodegradation are related to the removal of PAHs by bacteria. Biosorption is a physico-chemical process involved in the sorption of chemical substances on a biological surface (Aksu, 2005). It has been found that some bacteria (Stringfellow and Alvarez Cohen, 1999), fungi (Raghukumar et al., 2006), algae (Chung et al., 2007), as well as extracellular polymers (EPS) (Pan et al., 2010) demonstrated high adsorption ability for PAHs. Chen et al. (2010) and Yesilada et al. (2010) reported that both biosorption and biodegradation contributed to

the removal of PAHs in aquatic environment. However, the cellular response to the pollutant exposure involved in this process has not been investigated thoroughly, which led to limited understanding of the mechanism of PAHs bio-treatment since this bioprocess is the metabolically mediated activity by microorganisms.

PAHs removal included not only biosorption and biodegradation, but also transport (Gao et al., 2014), however, which step was the rate-limiting reaction remained to be further studied. PAHs transport through cells could cause membrane and cytoplasm accumulation (Ren et al., 2010). Transport and biodegradation were metabolically mediated activities (Gao et al., 2014), thus it is critical to determine the relation between biodegradation and cellular responses. Previous researches have shown that the toxicity of organic compounds influenced cell surface hydrophobicity (CSH) (Kaczorek et al., 2010), membrane permeability (Shi et al., 2013) and cell activity (Chen et al., 2014) during biodegradation. However, the influence of organic compounds on cell growth cycle, cell viability, cell size and internal granule which directly represented cellular characteristics during pollutant degradation process is still poorly understood. Revealing the interactions between PAHs treatment and cellular responses will help to accelerate PAHs degradation and further elucidate degradation mechanism.

The objective of the current study is to explore the relative

* Corresponding authors.

E-mail addresses: huayin@scut.edu.cn (H. Yin), jsye@jnu.edu.cn (J. Ye).

contributions of biosorption, biodegradation, accumulation and transport to the removal of pyrene by *Brevibacillus brevis*, along with cellular responses caused by pollutant by means of scanning electron microscope (SEM) and flow cytometry (FCM), aiming to more thoroughly reveal the mechanism of contaminant uptake in microbial remediation.

2. Materials and methods

2.1. Strain and chemicals

B. brevis, a potential strain for pyrene biodegradation used in this study, was isolated from the contaminated sediment samples collected at Guiyu in Guangdong Province, China (Ye et al., 2014).

Pyrene was obtained from Sigma-Aldrich (St. Louis, MO, USA). Beef extract medium (BEM) used for strain culture contained (g/L) 3 beef extracts, 10 peptone and 5 NaCl. Mineral salt medium (MSM) used as the degradation medium consisted of (mg/L) 50 K₂HPO₄, 30 KH₂PO₄, 10 MgSO₄·7H₂O and 50 C₆H₅Na₃O₇·2H₂O, and pH was adjusted to 7.0. All the mediums were previously sterilized in an autoclave at 121 °C for 30 min.

2.2. Microbial culture

B. brevis was inoculated into BEM at 30 °C on a rotary shaker at 130 r/min for 24 h. Subsequently, the cells were separated by centrifugation at 6000g for 10 min, and washed three times with sterile distilled water before usage in further experiments.

2.3. Biodegradation of pyrene

A stock solution (100 mg/L) of pyrene was dissolved in dichloromethane. The required quantities of this solution were transferred into 50 mL flasks containing 20 mL MSM to obtain 1 mg/L of pyrene concentration. These flasks capped with gauze were kept in a fume hood to allow the solvent to evaporate. Losses in pyrene content by volatilization were negligible in this process. *B. brevis* of 1 g/L were added after evaporation of the solvent. Then the flasks were incubated in the dark at 30 °C on a rotary shaker at 130 r/min for 1, 2, 4, 8, 24, 48, 72, 96, 120, 144, and 168 h. After that the cells were separated by centrifugation at 6000g. Residual pyrene in the supernatant was detected to determine the removal amount, and the total residual pyrene in the supernatant and cells was used to determine the biodegradation amount. To clarify the trend of pyrene transport and intracellular accumulation, the cells were washed with phosphate buffer solution (PBS, composition (g/L): 8.00 NaCl, 0.20 KCl, 1.42 Na₂HPO₄, 0.27 KH₂PO₄, pH 7.0) three times. Pyrene in PBS was detected to determine the residual pyrene on cell surface. Subsequently, the cells were resuspended in PBS (10 mL) by ultrasonication for 30 min. The supernatant centrifuged at 10,000g was used to determine the intracellular pyrene.

After cells were disrupted by ultrasonic pulverizer, the deposits were collected and suspended in 5 mL methanol, and then kept disrupting by ultrasonic pulverizer until the cell membrane was completely dissolved. The supernatant after centrifugation at 10,000g was used to determine the pyrene concentration in membrane (Li et al., 2007; Ren et al., 2010).

2.4. Biosorption of pyrene

To determine the passive attraction of pyrene by cell surface, biosorption was performed with cells inactivated by 2.5% glutaraldehyde for 36 h. The flasks with 20 mL MSM containing 1 mg/L pyrene and 1 g/L inactivated *B. brevis* were inoculated in the dark at 30 °C on a rotary shaker at 130 r/min for 1, 2, 4, 8, 24, 48, 72, 96,

120, 144, and 168 h, separately. Then the cells were separated by centrifugation at 6000g. The total residual pyrene in cells was used to estimate the biosorption amount.

2.5. Effect of pyrene on membrane permeability of *B. brevis*

Membrane permeability of *B. brevis* was determined by measuring the release of β-galactosidase into the medium using *o*-nitrophenyl-β-D-galactoside (ONPG) as a substrate (Ye et al., 2014).

2.6. Analytical method of pyrene

The residual pyrene in samples was extracted by ethyl acetate (Mahanty et al., 2008) and analyzed by high-performance liquid chromatography (HPLC) with UV detector at 254 nm and C18 reverse-phase column (dimensions 0.25 mm × 150 mm), methanol-water (90/10, v/v) was used with a flow rate of 1 mL/min as a mobile phase. The injection volume was 20 μL (Chen et al., 2014). Detection limit of pyrene was 0.5 μg/L.

2.7. SEM analysis of cellular surface morphology

After pyrene degradation, cells were fixed and dehydrated firstly, then added on the cover glass, drying in the CO₂ vacuum for 4 h. After that, the samples were coated with gold to strengthen the conductivity and photographed by scanning electron microscopy (PHILIPS XL-30E SEM).

2.8. Flow cytometry analysis

After pyrene degradation, one part of cells were collected and washed twice with sterile distilled water, and then transferred to the special FACS compatible BD TrueCount™ tubes containing known number of fluorescent beads (50,003 events). The samples were mixed gently and analyzed with flow cytometry immediately.

Another part of the cells were washed twice with sterile 0.1 M PBS, and then resuspended in 0.1 M PBS to obtain a cell concentration of approximately 10⁶ cells per milliliter (Chen et al., 2014). Subsequently, the cells were stained with propidium iodide (PI) for 10 min and analyzed with a FACS Aria flow cytometer (Becton Dickinson Corp., USA).

2.9. Statistical analysis

All of the experiments were performed in triplicate, and the mean values were used in the calculations. The standard deviations for all measurements ranged from 0.5% to 8.0%.

3. Results and discussion

3.1. Pyrene removal and biosorption

PAHs removal included not only biosorption and biodegradation, but also transport and accumulation. In this study, the amount of pyrene removal, biodegradation and biosorption were measured individually to illustrate the relations among these biological processes.

To reveal the contribution of metabolism-independent biosorption to pyrene removal, pyrene adsorption by cells inactivated by 2.5% glutaraldehyde was conducted. Fig. 1 shows that 0.32 mg/L pyrene was adsorbed within 24 h, and the biosorption amount slowly increased thereafter to 0.41 mg/L on the 168th hour. This result indicated that pyrene biosorption was primarily dependent on the physicochemical interactions between pyrene and *B. brevis*.

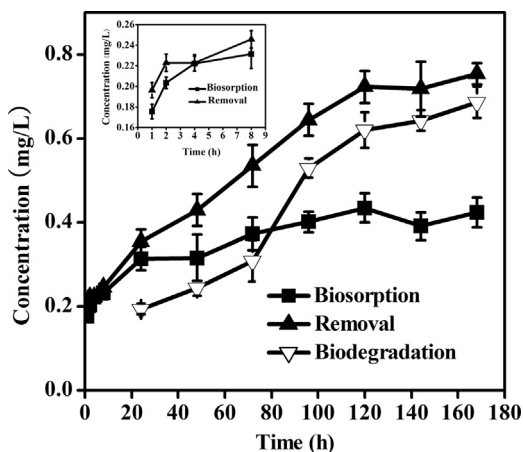


Fig. 1. Pyrene removal and biodegradation by *B. brevis*, and biosorption by inactivated *B. brevis*.

Active groups on the cell surface for pyrene binding were quickly occupied during the initial rapid phase. This is consistent with what obtained in triphenyltin biosorption by *Stenotrophomonas maltophilia* (Gao et al., 2014). The FTIR analysis of inactivated *B. brevis* with/without pyrene exposure was performed to ascertain the active groups possibly involved in the biosorption process on cell surface (see Fig. S1 in Supplementary material). The result suggested that organic phosphate, carboxyl and hydroxyl were predominant contributors in pyrene biosorption. As these active groups became occupied and pyrene in solution decreased, the chances of residual pyrene to contact cells reduced accordingly, which correlated with the subsequent slow increase in pyrene biosorption with time. This result further revealed that pyrene biosorption mainly occurred at the early stage of pyrene removal.

Fig. 1 demonstrates that pyrene removal was far higher than biosorption after 48 h. The removal of pyrene continued to rise to 0.75 mg/L on the 168th hour, increasing the disparity between removal and biosorption. This finding further implied that the removal process was dominated by either biodegradation or bioaccumulation. It is also shown in Fig. 1 that pyrene biodegradation was low initially, with only 0.19 mg/L at 24 h, but subsequently ascended to 0.69 mg/L at 168 h, which was very close to that of pyrene removal at the same period of time. This finding confirmed that pyrene removal was gradually dependent on biodegradation. This was in accordance with the result obtained in

triphenyltin removal by *S. maltophilia*, in which biodegradation gradually prevailed in removal process (Gao et al., 2014).

Furthermore, pyrene removal was more significant than biodegradation at the initial stage, which was likely to be caused by the transport and intracellular accumulation of pyrene. To verify these inferences, the following experiments separately examined the contribution of transport and accumulation to pyrene removal.

3.2. Distribution of pyrene in bacterial cells

In order to explore the interrelation of cells with pyrene, the cellular morphology after ultrasonication was observed through SEM analysis (see Fig. S2 in Supplementary material). It was found that there were no intact cells left. The fact that using deposits after ultrasonication as inocula showed no growth on BEM plate 24 h later further confirmed that cells were all broken (see Fig. S3 in Supplementary material). These results inferred that the intracellular pyrene content could be detected after cell disruption by ultrasonication. The residual pyrene in cytoplasm and on the surface of *B. brevis* with time is presented in Fig. 2a. Pyrene adsorbed by the cell surface reached its peak value of 0.06 mg/L at 24 h, which confirmed the result in Section 3.3.1 that surface adsorption played a role at the early stage of pyrene removal. It was seen that pyrene on the cell surface was low after 24 h (Fig. 2a), but a fast rising trend of the intracellular pyrene was observed at 24–72 h. This suggested that little pyrene was adsorbed by the cell surface; instead, more was transported into cytoplasm, leading to higher pyrene removal than biodegradation initially. After 168 h, the residual pyrene in cytoplasm declined to 0.09 mg/L, indicating that due to the action of related enzymes, such as catechol dioxygenase (Singh et al., 2013), peroxidase (Veignie et al., 2004) and superoxide dismutase (Schmidt et al., 2009), part of pyrene was degraded intracellularly.

Fig. 2b further implies that pyrene could accumulate in the membrane in a relatively short time, and then it was transported into cell through the membrane with the extension of time, as pyrene in the membrane declined to 0.093 mg/L at 168 h. Lipophilic hydrocarbons were preferably enriched in the microbial membrane when interacting with cells, thus increasing membrane fluidity and enhancing cell permeability (Ren et al., 2010). Due to high lipid solubility of pyrene and the electrostatic potential of molecular surface, membrane phospholipids interacted with pyrene by hydrophobic bond (Le Bourvellec and Renard, 2005), which formed stable conjugates. Therefore, membrane permeability

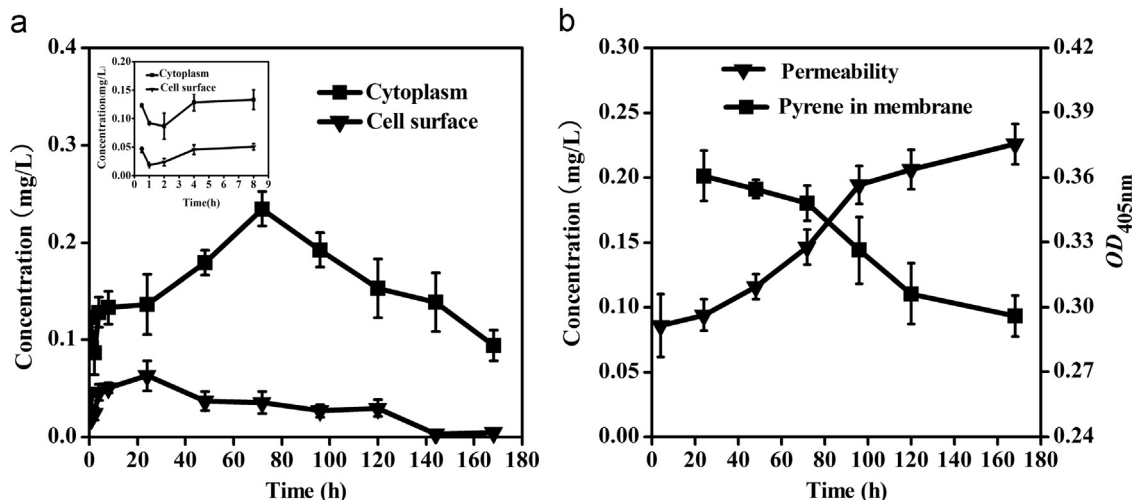


Fig. 2. Distribution of pyrene in cells of *B. brevis*: (a) distribution of pyrene in cytoplasm and on cell surface of *B. brevis* and (b) concentration of pyrene on membrane, and cellular membrane permeability during pyrene removal.

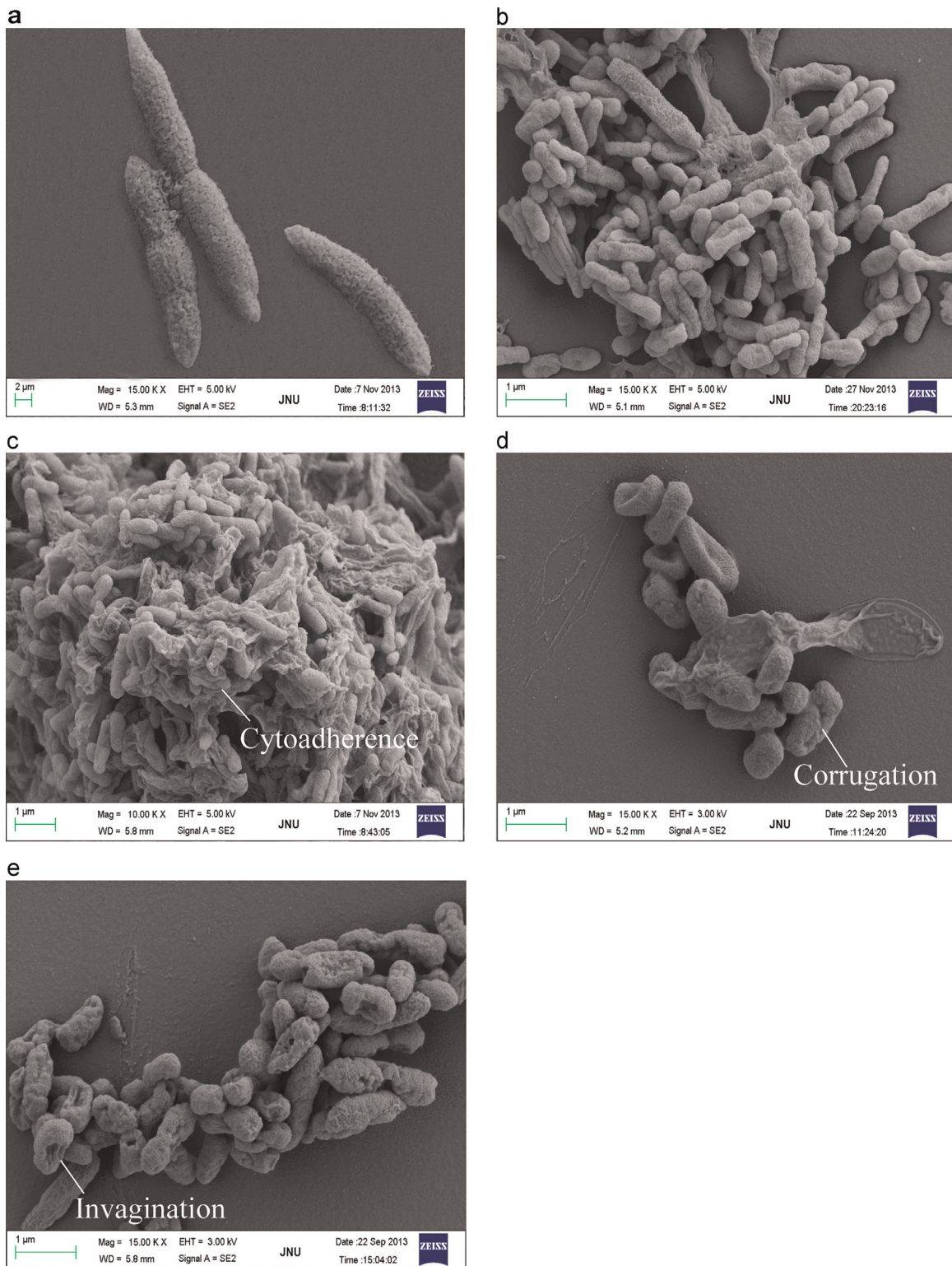


Fig. 3. Surface morphology of *B. brevis* before and after pyrene degradation: (a) stands for *B. brevis* in BEM after 24 h; (b) represents *B. brevis* in MSM after 48 h; (c)–(e) depicts *B. brevis* after degradation of 1 mg/L pyrene for 48 h, 120 h and 168 h, respectively.

increased accordingly. Besides, as cell wall and plasma membrane were the first barriers for microbe to decompose pollutants, pyrene accumulated in membrane would be hindered to go further inside the cell through transmembrane transport (Gokel George and Daschbach, 2007). Nevertheless, in this study, the residual pyrene in both extracellular MSM and membrane declined gradually, and pyrene did not accumulate largely in cytoplasm during

degradation, implying that the transmembrane transport of pyrene proceeded smoothly and pyrene was degraded continuously.

3.3. Analysis of surface morphology of *B. brevis*

As shown in Fig. 3, when compared to the cells in BEM (Fig. 3a) and MSM (Fig. 3b) without pyrene, the cell surface morphology

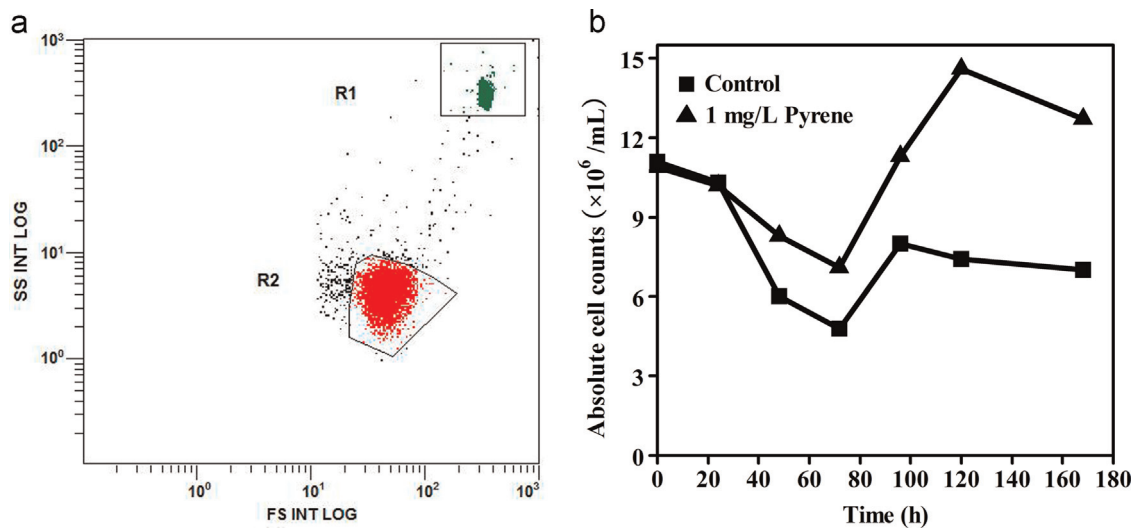


Fig. 4. Effect of pyrene on growth of *B. brevis*: (a) gating strategy used to define absolute cell counts by the TruCOUNT assay and (b) quantification of *B. brevis* over degradation time.

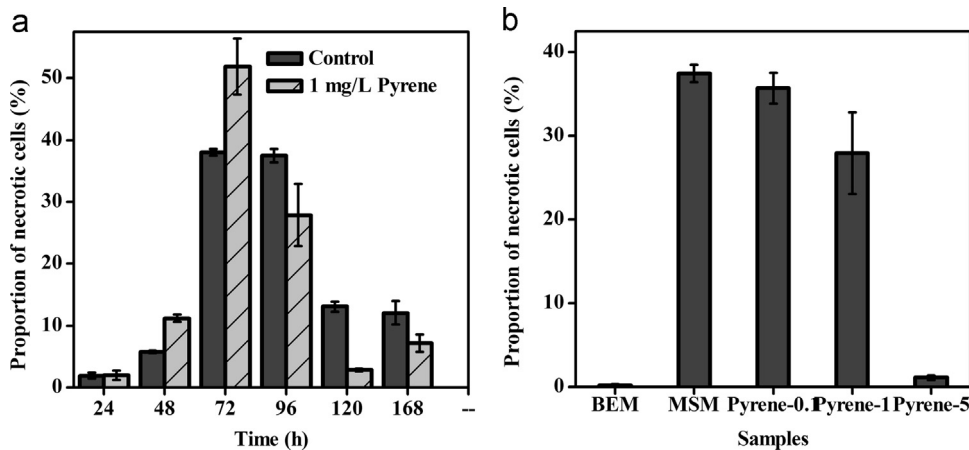


Fig. 5. Effect of pyrene on viability of *B. brevis*: (a) proportion of necrotic cells of *B. brevis* with increasing time, in system with MSM and pyrene (1 mg/L) and (b) proportion of necrotic cells of *B. brevis* in system with BEM, MSM, and pyrene at 0.1, 1 and 5 mg/L, respectively.

was affected severely by pyrene, with cytoadherence (Fig. 3c), cell surface corrugation (Fig. 3d) and cell invagination (Fig. 3e). Pyrene increased membrane permeability or triggered apoptosis in certain cells. Consequently, the structure of cell wall and membrane changed and partial outflow of the intracellular materials such as ions, proteins and sugars (Gao et al., 2014) appeared. However, the surface morphology of cells was largely intact. The experimental phenomena obtained here also confirmed the findings presented in our previous section of this study that ascending trend of pyrene removal began to slow down after 120 h. At this time, due to change of cell morphology, the adhesion of cell wall and membrane was affected, which was detrimental to the contact of residual pyrene with cells. Consequently, the removal capability of pyrene fell to a certain extent. Whereas, cells with integrated structure were still able to multiply and grow, producing some corresponding enzymes to degrade pyrene. Under pollutant stress, some microbes possessed resistance mechanisms, such as superoxide dismutase and metallothionein (Schmidt et al., 2009). Therefore, when extending contact time, pyrene removal could still increase accordingly.

3.4. Effect of pollutant on cell growth

TruCOUNT assay, which has been used for blood cell counting,

provides precise and reproducible cell quantification (Vuckovic et al., 2004). Fig. 4a shows the gating strategy for *B. brevis* and TruCOUNT™ beads. *B. brevis* was acquired in R2, with R1 as the TruCOUNT™ beads gate. The number of cells was calculated by the following formula (Sahu et al., 2013):

$$\text{Cell number} = (\text{events in R2}) \times (\text{number of beads per tube}) / \text{events in R1} \quad (1)$$

A significantly larger absolute cell number in the pollutant system after 96 h was exhibited by means of TruCOUNT assay, when compared with that of the control system (Fig. 4b). This finding revealed that the inhibitory effect of pyrene stress on cell metabolic activity was lower than that of the starvation in the control, in which no exogenous organic carbon existed. When analyzing the absolute cell counts obtained in this pollutant containing system, it was found that the figure shifted upward after 96 h (Fig. 4b), verifying that cells could regrow without adding new nutrients. As a *Bacillus* species, *B. brevis* could form endospores and release it. After 72 h, disruption of some cells or increase of membrane permeability enhanced the release of Na^+ , NO_3^- , NO_2^- , NH_4^+ , PO_4^{3-} , SO_4^{2-} and proteins (Gao et al., 2014; Tang et al., 2014). The cells and endospores were capable of utilizing these materials as energy source for further growth and

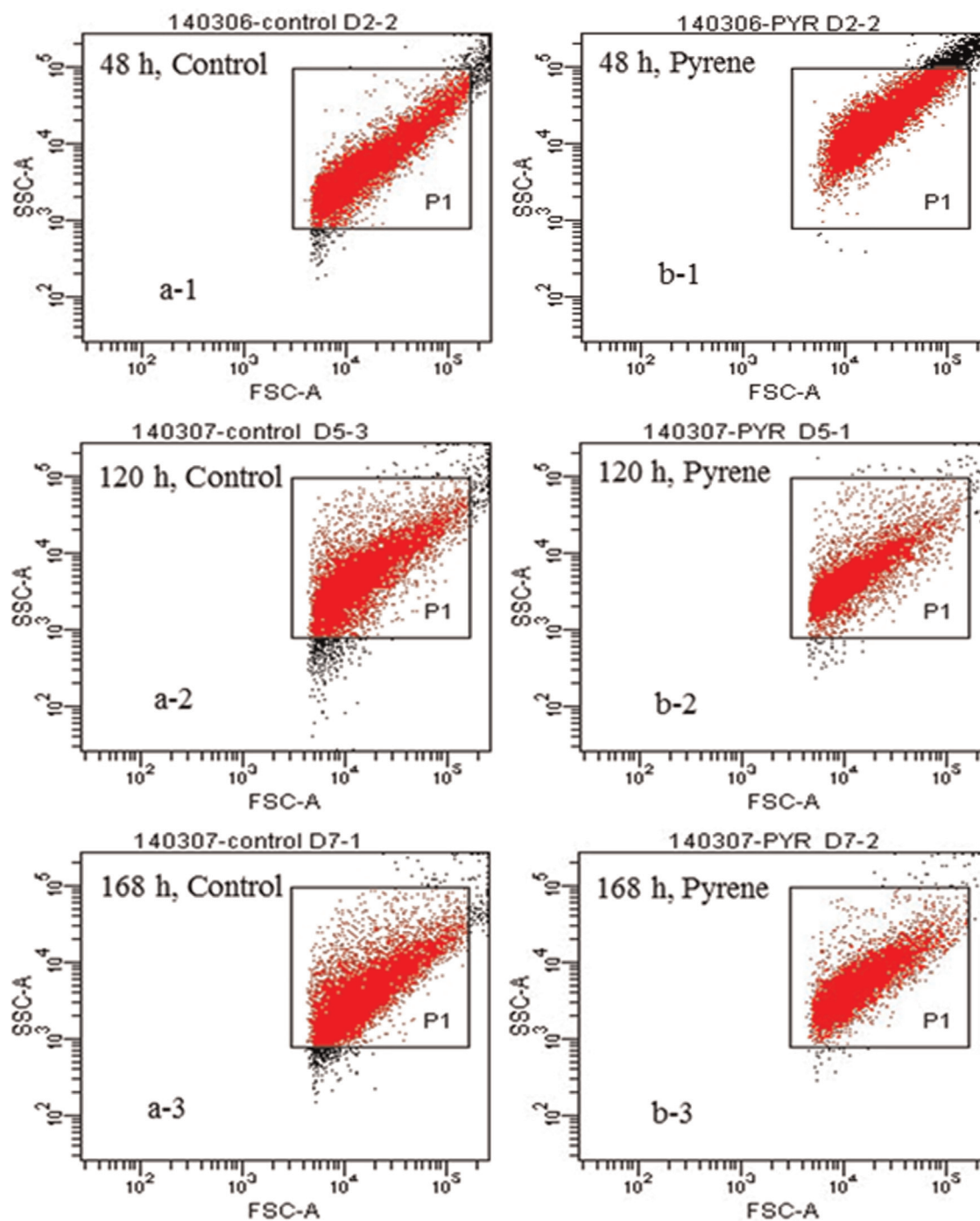


Fig. 6. Influence of pyrene on the cellular characteristics of *B. brevis*: a-1 to a-3 stands for the changes of cellular size and density in control system after 48, 120 and 168 h; b-1 to b-3 depicts the changes of size and density of cells that have interacted with pyrene (1 mg/L) for 48, 120 and 168 h, respectively.

reproduction (Aouadhi et al., 2013). Among these materials, NO_2^- was assimilated by nitrate reductase; the utilization of PO_4^{3-} was performed by an intracellular phosphorylative pathway (Tang et al., 2014); Na^+ was involved in the energy metabolism of bacteria; and SO_4^{2-} usually participated in electron accepting processes (Schreiber et al., 2004).

3.5. Effect of pollutant on viability of cells

In order to explore whether pyrene affected cell viability during degradation process, additional experiments were designed to detect necrotic cells after pyrene treatment by PI dye. When cells

are damaged, PI dye can go through the membrane to trigger red fluorescence which can be detected by FCM (Chen et al., 2014). The results in Fig. 5a showed that proportion of necrotic cells in both pyrene and control system turned downward up to 120 h, on account of the fact that *B. brevis* has adapted to the surroundings. This finding further confirmed that *B. brevis* formed spores intracellularly under nutrients-limited condition and spores utilized released intracellular materials in the solution as energy source for growth. Thus intact cells still accounted for the vast majority of *B. brevis* after 120 h. Although SEM observation showed that cell surface morphology was affected by pyrene, these intact cells continued to produce corresponding enzymes to degrade pyrene.

Therefore, pyrene removal could still increase after 120 h.

The mortality of cells in pyrene containing system was only 2.8% after 120 h (Fig. 5a), which was much lower than the control (13.5%). This implied that *B. brevis* might utilize pyrene as carbon source. There were two ways for microorganisms to degrade PAHs, either by utilizing PAHs as the only carbon and energy source or by assimilating an alternative carbon source. To date, only a few isolates have been reported to be able to degrade PAHs by utilizing it as a sole carbon source (Chen et al., 2013; Juhasz et al., 2000). It is evident from Fig. 5b that *B. brevis* could make the best of pyrene as a sole carbon source. The proportion of necrotic cells of *B. brevis* after dealing with pollutant, especially with high level pyrene for 96 h, was apparently lower than that in MSM system. When pyrene concentration was 5 mg/L, only 1.3% necrotic cells occurred in pollution system, closing to the mortality in nutrient medium system. The results indicated that *B. brevis* could utilize relative high level pyrene for growth and metabolism to a certain extent. This finding was consistent with previous investigations that white-rot fungi utilized pyrene as carbon source (Chen et al., 2010).

3.6. Effect of pollutant on characteristics of cells

The common kinds of scattered light to be utilized during FCM analysis are forward scattering (FSC) and side scattering (SSC). FSC–SSC diagram during FCM analysis can help to determine cellular characteristics, as FSC is closely related to the square of the cell diameter and SSC represents intracellular particle density (Czechowska et al., 2008; Chen et al., 2014). It was found that cell population in both pollutant and control systems changed obviously after 120 h, with the bacterial cells scattering (Fig. 6). The SSC value in the control was smaller compared with that in the pollution system, which revealed that more cell cytoplasm was released in the system without pyrene (Chen et al., 2014). Our previous investigation also verified that *B. brevis* could utilize pyrene as carbon source for growth, which manifested as more plump cells than the control ones after dealing with pyrene.

In comparison with the same system, it was found that cell size in pollutant system decreased with the ascending time, with the FSC value becoming smaller. And the internal structure of bacterial cells changed after 120 h as SSC value decreased. Combined with the results of SEM, the collapse of cell structure after 120 h was severe. This implied that pyrene greatly affected the cell of *B. brevis*. Cell membrane functioned in regulating osmotic pressure, enzymatic reaction and material transport (Ye et al., 2014). The exposure of *B. brevis* to pyrene increased the cell membrane permeability after 48 h, which caused intracellular materials such as ions, proteins and sugars to be easily released to the MSM. Therefore, cell size and intracellular particle density decreased over incubation time.

4. Conclusions

Pyrene was initially adsorbed by *B. brevis* and subsequently transported across the plasma membrane into the cell. Then, part of pyrene was degraded under the action of related enzymes, yet another small part of it still accumulated intracellularly. During this process, pyrene removal was primarily dependent on biodegradation. Although the presence of pyrene affected surface morphology of cell, *B. brevis* could utilize pyrene as carbon source for growth, and cells regrew after 96 h. Moreover, proportion of necrotic cells in pyrene containing system was only 2.8% after 120 h, and cell size and intracellular particle density changed, due to the influence of contaminant.

Acknowledgment

The authors would like to thank the National Natural Science Foundation of China (Nos. U0933002, 50978122, and 41330639), Natural Science Foundation of Guangdong Province, China (S2013020012808), and the Fundamental Research Funds for the Central Universities (No. 2013ZM0126) for the financial support of this work.

Appendix A. Supplementary material

Supplementary data associated with this article can be found in the online version at <http://dx.doi.org/10.1016/j.ecoenv.2015.02.015>.

References

- Aksu, Z., 2005. Application of biosorption for the removal of organic pollutants: a review. *Process Biochem.* 40, 997–1026.
- Aouadhi, C., Simonin, H., Maaroufi, A., Mejri, S., 2013. Optimization of nutrient-induced germination of *Bacillus sporothermodurans* spores using response surface methodology. *Food Microbiol.* 36, 320–326.
- Chen, B.L., Wang, Y.S., Hu, D.F., 2010. Biosorption and biodegradation of polycyclic aromatic hydrocarbons in aqueous solutions by a consortium of white-rot fungi. *J. Hazard. Mater.* 179, 845–851.
- Chen, S.N., Yin, H., Ye, J.S., Peng, H., Zhang, N., He, B.Y., 2013. Effect of copper(II) on biodegradation of benzo[a]pyrene by *Stenotrophomonas maltophilia*. *Chemosphere* 90, 1811–1820.
- Chen, S.N., Yin, H., Ye, J.S., Peng, H., Liu, Z.H., Dang, Z., Chang, J.J., 2014. Influence of co-existed benzo[a]pyrene and copper on the cellular characteristics of *Stenotrophomonas maltophilia* during biodegradation and transformation. *Bioresour. Technol.* 158, 181–187.
- Chung, M.K., Tsui, M.T.K., Cheung, K.C., Tam, N.F.Y., Wong, M.H., 2007. Removal of aqueous phenanthrene by brown seaweed *Sargassum hemiphyllum*: sorption-kinetic and equilibrium studies. *Sep. Purif. Technol.* 54, 355–362.
- Czechowska, K., Johnson, D.R., Meer, J.R., 2008. Use of flow cytometric methods for single-cell analysis in environmental microbiology. *Curr. Opin. Microbiol.* 11, 205–212.
- Das, K., Mukherjee, A., 2007. Differential utilization of pyrene as the sole source of carbon by *Bacillus subtilis* and *Pseudomonas aeruginosa* strains: role of bio-surfactants in enhancing bioavailability. *J. Appl. Microbiol.* 102, 195–203.
- Dissanayake, A., Piggott, C., Baldwin, C., Sloman, K.A., 2010. Elucidating cellular and behavioural effects of contaminant impact (polycyclic aromatic hydrocarbons, PAHs) in both laboratory-exposed and field-collected shore crabs, *carcinus maenas* (Crustacea; Decapoda). *Mar. Environ. Res.* 70, 368–373.
- Gao, J., Ye, J.S., Ma, J.W., Tang, L.T., Huang, J., 2014. Biosorption and biodegradation of triphenyltin by *Stenotrophomonas maltophilia* and their influence on cellular metabolism. *J. Hazard. Mater.* 276, 112–119.
- Gokel George, W., Daschbach, M.M., 2007. Coordination and transport of alkali metal cations through phospholipid bilayer membranes by hydrophilic channels. *Coord. Chem. Rev.* 252, 886–902.
- Juhasz, A.L., Stanley, G.A., Britz, M.L., 2000. Microbial degradation and detoxification of high molecular weight polycyclic aromatic hydrocarbons by *Stenotrophomonas maltophilia* strain VUN 10.003. *Lett. Microbiol.* 30, 396–401.
- Kaczorek, E., Urbanowicz, M., Olszanowski, A., 2010. The influence of surfactants on cell surface properties of *Aeromonas hydrophila* during diesel oil biodegradation. *Colloids Surf. B: Biointerfaces* 81, 363–368.
- Le Bourvellec, C., Renard, C.M.G.C., 2005. Non-covalent interaction between proeyanidins and apple cell wall material. Part II: quantification and impact of cell wall drying. *Biochim. Biophys. Acta* 1725, 1–9.
- Li, L., Gao, H.W., Ren, J.R., Chen, L., Li, Y.C., Zhao, J.F., Zhao, H.P., Yuan, Y., 2007. Binding of Sudan II and IV to lecithin liposomes and *E. coli* membranes: insights into the toxicity of hydrophobic azo dyes. *BMC Struct. Biol.* 7, 16.
- Mahanty, B., Pakshirajan, K., Venkata Dasu, V., 2008. Biodegradation of pyrene by *Mycobacterium frederiksbergense* in a two-phase partitioning bioreactor system. *Bioresour. Technol.* 99, 2694–2698.
- Oliveira, M., Gravato, C., Guilhermino, L., 2012. Acute toxic effects of pyrene on *Pomatoschistus microps* (Teleostei, Gobiidae): mortality, biomarkers and swimming performance. *Ecol. Indic.* 19, 206–214.
- Pan, X., Liu, J., Zhang, D., 2010. Binding of phenanthrene to extracellular polymeric substances (EPS) from aerobic activated sludge: a fluorescence study. *Colloids Surf. B* 80, 103–106.
- Raghukumar, C., Shailaja, M.S., Parameswaran, M.S., Singh, S.K., 2006. Removal of polycyclic aromatic hydrocarbons from aqueous media by the marine fungus NIOCC#312: involvement of lignin-degrading enzymes and exopolysaccharides. *Ind. J. Mar. Sci.* 35, 373–379.
- Ren, J.R., Zhao, H.P., Song, C., Wang, S.L., Li, L., Xu, Y.T., Gao, H.W., 2010. Comparative transmembrane transports of four typical lipophilic organic chemicals.

- Bioresour. Technol. 101, 8632–8638.
- Sahu, U., Sahoo, P.K., Kar, S.K., Mohapatra, B.N., Ranjit, M., 2013. Association of TNF level with production of circulating cellular microparticles during clinical manifestation of human cerebral malaria. *Hum. Immunol.* 74, 713–721.
- Schmidt, A., Haferburg, G., Schmidt, A., Lischke, U., Merten, D., Ghergel, F., Büchel, G., Kothe, E., 2009. Heavy metal resistance to the extreme: *Streptomyces* strains from a former uranium mining area. *Chem. Erde – Geochem.* 69, 35–44.
- Schreiber, M.E., Carey, G.R., Feinstein, D.T., Bahr, J.M., 2004. Mechanisms of electron acceptor utilization: implications for simulating anaerobic biodegradation. *J. Contam. Hydrol.* 73, 99–127.
- Shi, G.Y., Yin, H., Ye, J.S., Peng, H., Li, J., Luo, C.L., 2013. Effect of cadmium ion on biodegradation of decabromodiphenyl ether (BDE-209) by *Pseudomonas aeruginosa*. *J. Hazard. Mater.* 263, 711–717.
- Singh, S.N., Kumari, B., Upadhyay, S.K., Mishra, S., Kumar, D., 2013. Bacterial degradation of pyrene in minimal salt medium mediated catechol dioxygenases: enzyme purification and molecular size determination. *Bioresour. Technol.* 133, 293–300.
- Stringfellow, W.T., Alvarez Cohen, L., 1999. Evaluating the relationship between the sorption of PAHs to bacterial biomass and biodegradation. *Water. Res.* 33, 2535–2544.
- Tang, S.Y., Bai, J.Q., Yin, H., Ye, J.S., Peng, H., Liu, Z.H., Dang, Z., 2014. Tea saponin enhanced biodegradation of decabromodiphenyl ether by *Brevibacillus brevis*. *Chemosphere.* 114, 255–261.
- Veignie, E., Rafin, C., Woisel, P., Cazier, F., 2004. Preliminary evidence of the role of hydrogen peroxide in the degradation of benzo[a]pyrene by a non-white rot fungus *Fusarium solani*. *Environ. Pollut.* 129, 1–4.
- Vuckovic, S., Gardiner, D., Field, K., Chapman, G.V., 2004. Monitoring dendritic cells in clinical practice using a new whole blood single-platform TruCOUNT assay. *J. Immunol. Methods* 284, 73–78.
- Ye, J.S., Zhao, H.J., Yin, H., Peng, H., Tang, L.T., Gao, J., Ma, W., 2014. Triphenyltin biodegradation and intracellular material release by *Brevibacillus brevis*. *Chemosphere* 105, 62–67.
- Yesilada, O., Yildirim, S.C., Birhanli, E., Apohan, E., Asma, D., Kuru, F., 2010. The evaluation of pre-grown mycelial pellets in decolorization of textile dyes during repeated batch process. *World J. Microbiol. Biotechnol.* 26, 33–39.